

A COMPACT BEAM RECONFIGURABLE ANTENNA FOR SYMMETRIC BEAM SWITCHING

W. Kang, K. H. Ko, and K. Kim*

School of Information and Mechatronics, Gwangju Institute of Science and Technology, Gwangju, Republic of Korea

Abstract—In this paper, two radiation pattern-reconfigurable antennas are designed to operate near the frequency of 1.8 GHz. The geometry of the proposed antennas is symmetric with respect to the vertical center line. The electrical shapes of the antennas are composed of a monopole-loaded loop and an open wire. The open wire functions as either a director or reflector for the two antennas. Depending on the switching state, the antennas can select between two beam directions with no input impedance difference. The sizes of each antenna are then optimized to achieve beam switching capability using PIN diodes and FETs. The reflection coefficients and gain patterns for two bias conditions using both switches are measured and compared with the simulated results. The measured results show that the proposed antennas can clearly alternate their beam directions using the switching components.

1. INTRODUCTION

Reconfigurable antennas, which offer diverse functions in frequency, radiation pattern, or polarization, have received significant attention in wireless communications [1–14]. Among these functions, alternating the antenna beam patterns may be especially useful because steering a beam toward the intended direction can avoid multi-path fading and interference in urban and indoor environments. Several antenna designs have been proposed in attempts to realize radiation pattern reconfiguration. In most radiation pattern-reconfigurable antennas found in literature, the antenna operating frequency varies as the radiation patterns are alternated [15–17], due to the fact that the

Received 20 March 2012, Accepted 11 June 2012, Scheduled 12 June 2012

* Corresponding author: Kangwook Kim (mkkim@gist.ac.kr).

geometry of the antenna varies for each switching state. In contrast, the antenna introduced in [3, 18] maintains its operating frequency while switching the radiation pattern. These antennas utilize parasitic elements such as a director and a reflector for pattern reconfiguration while the electrical shape of the driven element remains the same; thus, the input impedance remains stable for every switching state. However, the size of these antennas may be too large ($\sim\lambda/2$) to be practical in mobile applications. As more compact and lighter devices are necessary in recent wireless applications, the size of the antenna may be another important issue [2, 19].

In this paper, two types of radiation-pattern reconfigurable antenna that can symmetrically alternate their beam directions are proposed. The proposed antennas are electrically compact and can select beam directions while maintaining essentially the same input impedance. The remainder of this paper is organized as follows. In Section 2, the operation mechanism of the proposed antennas is explained based on the fundamental structure. The structures are composed of a loop and an open wire; the open wire is shown to serve as either a director or a reflector for both types. In Section 3, the antennas are practically designed by replacing the lower portion of the fundamental structure with the ground and equipping the antennas with tunable switching devices. In Section 4, the antennas are implemented such that they operate over DCS 1800 frequency bands [20] and their performance measured. The simulated and measured results are in a good agreement, showing beam pattern reconfigurability.

2. FUNDAMENTAL STRUCTURE OF THE PROPOSED ANTENNA

Figures 1(a) and (b) show the fundamental structures of the proposed antenna. The antennas are each composed of a dipole and two bracket-shaped wires; the switches are located at the top and bottom ends of both wires. Depending on the switching state, only one wire is connected to the dipole to form a loop and the other wire is disconnected. As shown in Fig. 1(c), a loop can be decomposed into loop and dipole modes [21]. For loop mode, the current I_l is anti-symmetric with respect to the vertical center (amplitudes are the same, but phases are different by π on either side). On the other hand, the dipole mode current I_d is symmetric with respect to the vertical center. Since the total current I is represented by $I = I_l + I_d$, the total radiated field can be obtained by superposing the two modes fields. The strengths of the radiated fields in the $+x$ and the $-x$ directions are

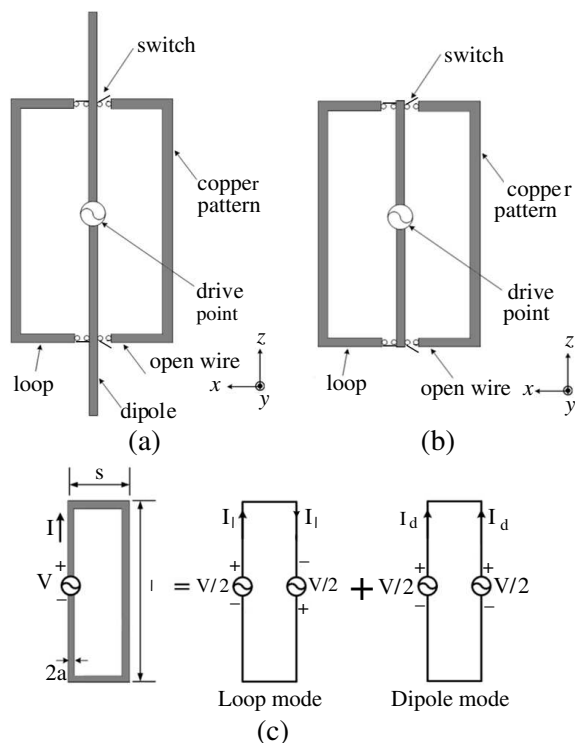


Figure 1. Fundamental structure of the proposed antenna, which consists of: (a) a dipole-loaded loop and an open wire, (b) a loop and an open wire, and (c) decomposition of a loop antenna into loop and dipole mode models.

consequently different, which leads to the directive radiation pattern shown in dotted lines Fig. 2(b). The figure shows that the pattern is slightly directive in the $-x$ direction [21]. The open wires in Figs. 1(a) and (b) modify the radiation pattern by behaving as either a director or reflector depending on the length of the open wire. Fig. 2 shows the directivity patterns of the fundamental antenna structures with and without the open wire. As shown in Fig. 2(a) (dotted lines), the directivity pattern of the dipole-loaded loop that does not contain an open wire is observed to be slightly stronger in the $-x$ direction. When an open wire exists nearby, the radiation pattern is modified. The directivity pattern of the dipole-loaded loop with a nearby open wire is represented in dashed lines. When the open wire is nearby a loop, where the wire is relatively shorter than the vertical length of the antenna, radiation in the $-x$ direction is seen to be much stronger than

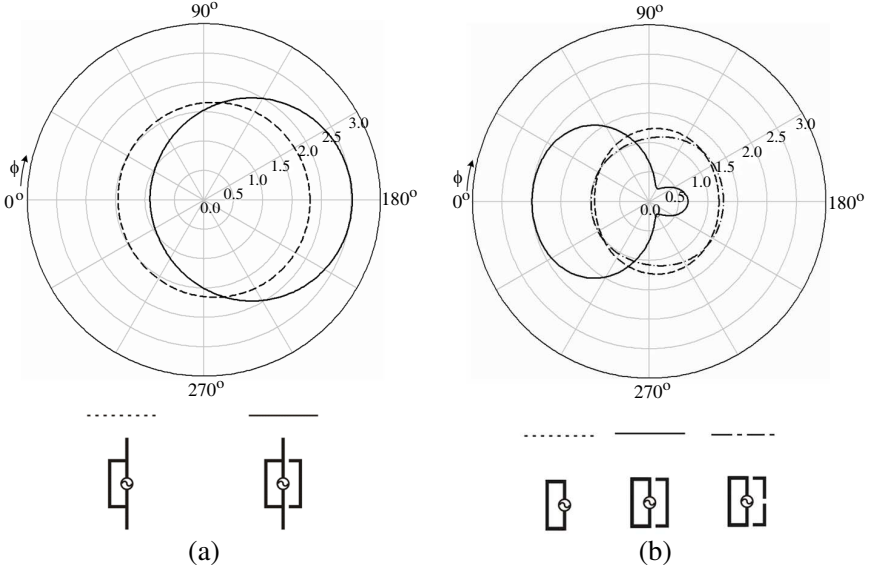


Figure 2. Directivity patterns of the antennas: (a) a dipole-loaded loop and open wire and (b) a loop and open wire.

in the $+x$ direction. Thus, the open wire in Fig. 1(a) can be considered to function as a director. Fig. 2(b) shows the directivity pattern of the loop with no open wire (dotted lines); the directivity pattern is slightly stronger in the $-x$ direction. On the other hand, when an open wire that is longer than the vertical length of the antenna is near a loop, the radiation pattern also changes, as represented in dashed lines. In this case, the radiation pattern in the $+x$ direction is observed to be much stronger than in the $-x$ direction. Thus, the open wire in Fig. 1(b) serves as a reflector. Fig. 2(b) also presents the directivity pattern of a loop with an open wire that is divided into two segments (dash-dot line). When the open wire is split into two segments, which are shorter than the vertical length of the antenna, the radiation pattern becomes almost analogous to that of the loop with no open wire. Thus, in this case, the two open wires cannot be regarded as a reflector. In summary, the radiation patterns in Fig. 2 show that a directive radiation pattern can be obtained by placing a wire near a loop. The electrical shape of the loop and wire can then be flipped about the vertical center axis using switching elements near the top and bottom centers of the antenna. Thus, the geometries in Fig. 1 can choose between the two beam directions.

3. PRACTICAL DESIGN OF FUNDAMENTAL STRUCTURE

Figure 3 illustrates the two proposed antennas in practical structures. The lower halves of both the antennas are replaced by a rectangular copper plate, which functions as the ground for both the RF and DC signals. These structures are more practical than the fundamental structures for two reasons. First, the size of the antennas is significantly reduced. Although the ground contributes to the radiation to a certain extent, it can be used to incorporate other circuit components. Thus, the area occupied by the antenna is only the upper portion of the fundamental structure. Second, in the practical structures, no baluns are necessary when the antennas are fed by an unbalanced source terminal since the grounded terminal is connected to the antenna ground. Note that in Fig. 3(b), extended monopoles are added to the bracket-shaped wires in order for the open wire to function more strongly as a reflector. The practical structures are then implemented on 0.8 mm-thick FR-4 ($\epsilon_r = 4.6$, $\tan \delta = 0.02$) printed circuit boards (PCBs). The ground is a 30 mm \times 44 mm copper-clad PCB. The length of the bare PCB is the same as the monopole length (L_{monopole}), and two semiconductor switching elements such as Microsemi MPP4203 PIN diodes or Agilent ATF-34143 FET switches are used [22–24]. Fig. 4 is the schematic of the connection diagrams, illustrating how the PIN diode and FET switches are connected in the antenna. In the figure, the thick lines represent the electrical paths, and V_c and v_s

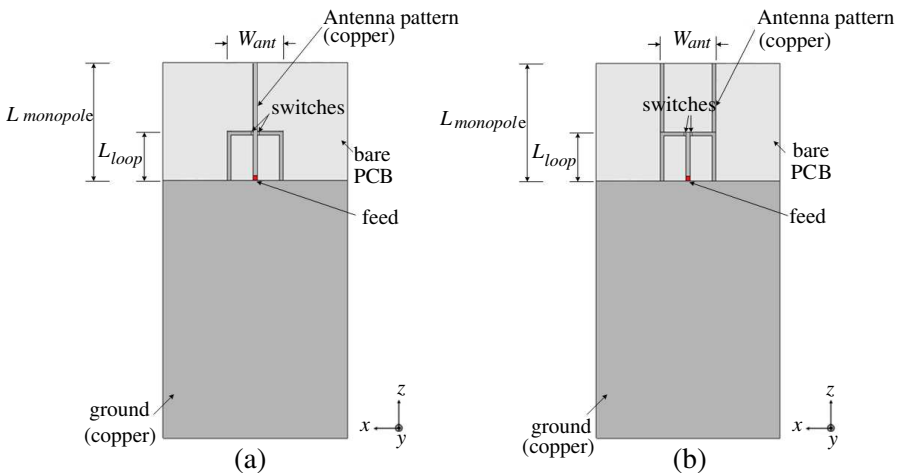


Figure 3. Geometries of the proposed antennas: (a) director-type and (b) reflector-type.

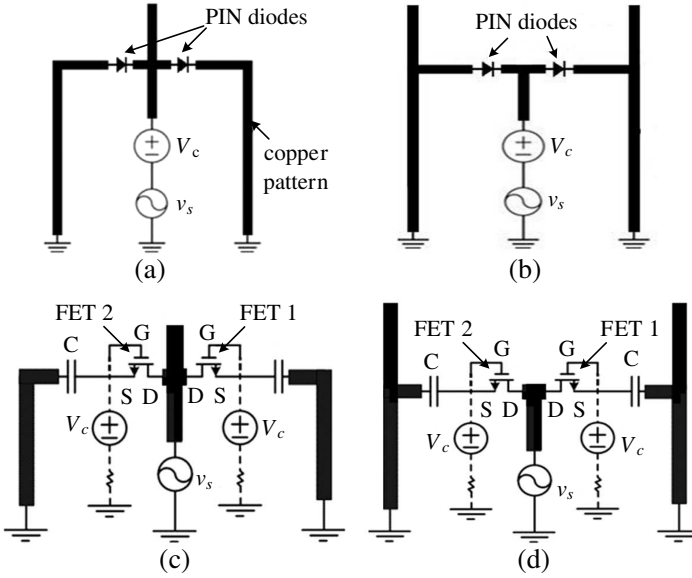


Figure 4. Schematic connection diagrams of (a) PIN diodes in director-type antenna, (b) PIN diodes in reflector-type antenna, (c) FET switches in director-type antenna, and (d) FET switches in reflector-type antenna.

represent the DC switch control voltage and the RF signal, respectively. The DC control voltage is obtained using a 1.5 V battery. By adjusting the direction of the battery connection, V_c can be either +1.5 V or -1.5 V. Note that in order to prohibit the DC current from flowing into the RF measurement system, the RF signal is connected to a DC block, which is omitted in Fig. 4. For antennas with PIN diode switches, both the DC control voltage and RF signal are simultaneously applied to the monopole in the center. Because the diodes are aligned in the same direction, only one diode is turned on depending on the DC voltage sign. In contrast, the DC control voltage is provided through separate control lines for antennas with FET switches, each connected to the gate of an FET. The control lines are loaded with a 500 Ω resistor, which suppresses the induced current on the line at the RF frequency in order to minimize the disturbance. Because the gate draws essentially no current, the DC power loss due to loading is negligible. Note that at the source of each FET, a 0.3 pF chip capacitor is connected in series; such a connection reduces the off-state capacitance, thereby allowing the antenna to operate at higher frequencies.

Since both types of switches used in this research are far from perfect, especially when operated at microwave frequencies, non-ideal

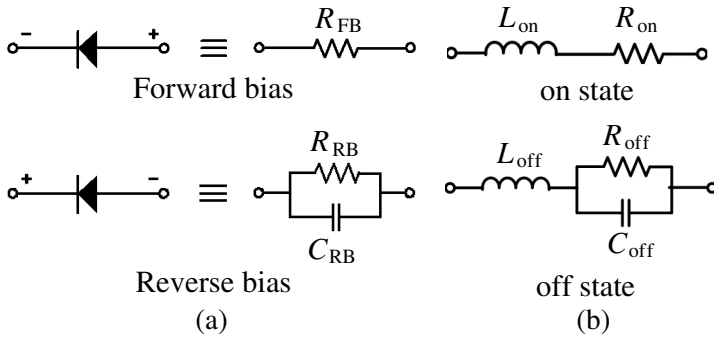


Figure 5. Equivalent linear circuit models of PIN diode (MPP4203) and FET switch (ATF-34143): (a) PIN diode with $R_{FB} = 3 \Omega$, $R_{RB} = 25 \text{ k}\Omega$, and $C_{RB} = 0.12 \text{ pF}$ (b) FET with $L_{on} = L_{off} = 2.6 \text{ nH}$, $R_{on} = 4.3 \Omega$, $R_{off} = 5.9 \text{ k}\Omega$, and $C_{off} = 0.49 \text{ pF}$.

effects of the switches are equivalently represented corresponding to both on and off states using linear circuit models. Fig. 5 shows the equivalent linear circuit models of the PIN diode and FET [22, 23]. Based on these models, a series of simulations is then performed to choose the dimensions of the two antennas controlled by the switches. The dimensions of the proposed antenna are determined such that the antenna has a large gain-bandwidth product and a sufficient front-to-back ratio (FBR). The FBR is defined as follows:

$$\text{FBR} = \frac{|\overline{E}_\Theta(\Phi = 0^\circ)|^2}{|\overline{E}_\Theta(\Phi = 180^\circ)|^2} \text{ if } |\overline{E}_\Theta(\Phi = 0^\circ)|^2 > |\overline{E}_\Theta(\Phi = 180^\circ)|^2$$

or

$$= \frac{|\overline{E}_\Theta(\Phi = 180^\circ)|^2}{|\overline{E}_\Theta(\Phi = 0^\circ)|^2} \text{ if } |\overline{E}_\Theta(\Phi = 180^\circ)|^2 > |\overline{E}_\Theta(\Phi = 0^\circ)|^2$$

In this paper, the minimum-allowable FBR is set at 4.8 dB, which corresponds to a linear ratio of 3. The detailed dimensions of the proposed antenna with PIN diode and FET are represented in Table 1.

4. IMPLEMENTATION AND MEASUREMENT

The antennas are implemented and characteristics measured through experiments. Fig. 6 compares the measured reflection coefficients of the antenna under different bias conditions with the simulated results over a frequency range between 1.0 and 3.0 GHz. The measured results for two switching states are represented in solid and dashed lines, respectively, while the dotted line represents the simulated results. The

Table 1. Detailed dimensions of the proposed antenna with tunable switches.

Antenna	Switch	W_{ant}	L_{ant}	L_{monopole}
Director type	PIN	12.5 mm	14.1 mm	28.2 mm
	FET	25 mm	8.8 mm	24.64 mm
Reflector type	PIN	21 mm	8.75 mm	22.75 mm
	FET	16.5 mm	10.68 mm	21.36 mm

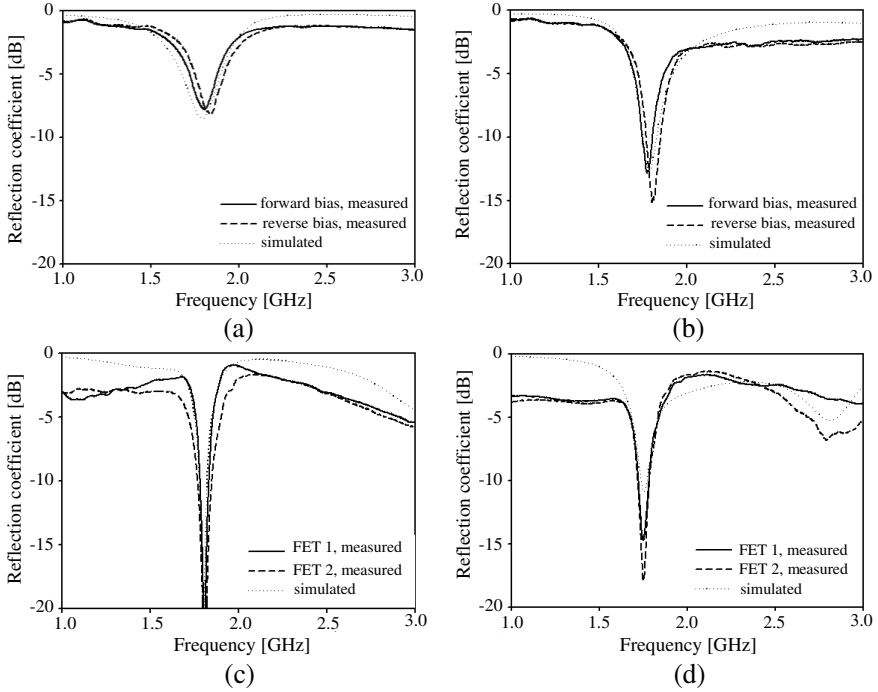
**Figure 6.** Simulated and measured reflection coefficients of (a) director-type antenna with PIN diodes, (b) reflector-type antenna with PIN diodes, (c) director-type antenna with FETs, and (d) reflector-type antenna with FETs.

figure indicates that the measured results agree well with the simulated results. Moreover, the measured results for the two switching states are observed to be essentially identical to each other, suggesting that the antenna preserves its input impedance, irrespective of the switching state. The 6 dB bandwidths are all measured to cover the DCS 1800 frequency band; the simulated and measured bandwidths are tabulated in Table 2.

Table 2. Simulated and measured 6 dB bandwidths of antennas with PIN diodes and FET switches.

Antenna type	Switch type	Simulated BW	Measured BW (Bias 1)	Measured BW (Bias 2)
Director type	PIN	171 MHz (1.701–1.872 GHz)	119 MHz (1.739–1.858 GHz)	122 MHz (1.772–1.894 GHz)
	FET	84 MHz (1.757–1.841 GHz)	81 MHz (1.766–1.847 GHz)	153 MHz (1.734–1.887 GHz)
Reflector type	PIN	184 MHz (1.709–1.893 GHz)	135 MHz (1.716–1.851 GHz)	157 MHz (1.738–1.895 GHz)
	FET	119 MHz (1.698–1.817 GHz)	124 MHz (1.692–1.816 GHz)	132 MHz (1.691–1.823 GHz)

*Bias1: forward bias (PIN diodes), FET1 on (FET's).

Bias2: reverse bias (PIN diodes), FET2 on (FET's).

Figures 7 and 8 show the measured and simulated gain patterns of antennas with PIN diodes and FET switches under different bias conditions. All patterns are observed at 1.8 GHz in the x - y plane when $\Theta = 90^\circ$; the measured and simulated results are represented in dashed and dotted lines, respectively. The patterns in the upper and lower rows show the gain patterns of director-type and reflector-type antennas. The patterns in the left and right columns show the patterns under forward and reverse bias conditions. The patterns are normalized by the maximum gain obtained in the simulation, and the measured results are seen to be in good agreement with the simulated results. In the case of director-type antennas, the radiation is stronger in the $+x$ direction ($\Phi = 0^\circ$) under forward bias conditions, while such a pattern symmetrically changes under reverse bias conditions, radiating stronger in the $-x$ direction ($\Phi = 90^\circ$). On the other hand, the reflector-type antenna radiates stronger in the $-x$ direction ($\Phi = 90^\circ$) under forward bias conditions, and in the $+x$ direction ($\Phi = 0^\circ$) under reverse bias conditions. The maximum gain and FBR of the antennas are tabulated in Table 3.

Note that in the proposed antenna, the operation as a loop mode may induce cross polarized radiation. In the simulated results, the minimum cross polarization discriminations are more than 11.41 dB, 2.49 dB, 3.46 dB, and 1.18 dB within the 3 dB beam width for director-type antenna with PIN diodes, reflector-type antenna with PIN diodes, director-type antenna with FETs, and reflector-type antenna with FETs, respectively. Thus, if such a cross polarized radiation leads to a

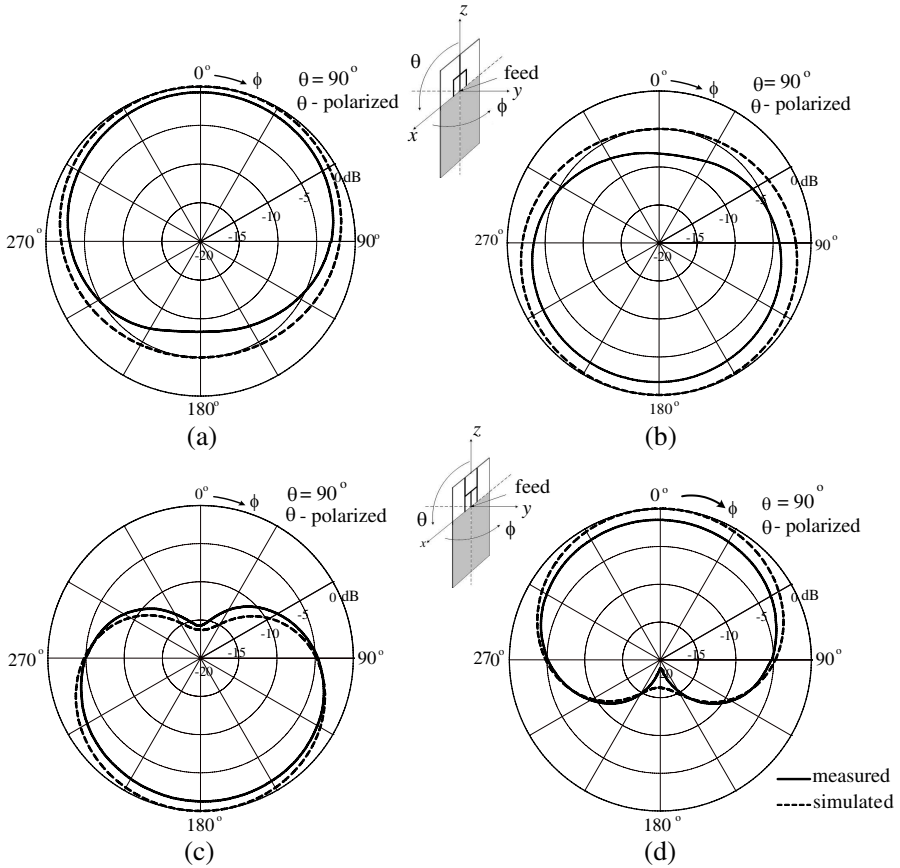


Figure 7. Simulated and measured gain patterns of the antennas with PIN diodes: (a) director-type, forward bias, (b) director-type, reverse bias, (c) reflector-type, forward bias, and (d) reflector-type, reverse bias.

problem in wireless communication systems, the director-type antenna with PIN diodes becomes regarded as the most suitable type.

Typically, semiconductor switches in the antenna have negative effects on the antennas radiation performance [25]. Ideally, the radiation efficiency of an antenna with switching devices should be the same as the antenna with hard-wired on/off switches. However, in reality, the finite resistances of the on and off-state switches lead to increased power consumption and thus deterioration in the antenna efficiency. Table 4 shows the computed antenna efficiency when the switch's on or off state resistances are idealized. In the table, the antenna efficiency used in this paper is defined as the conduction-

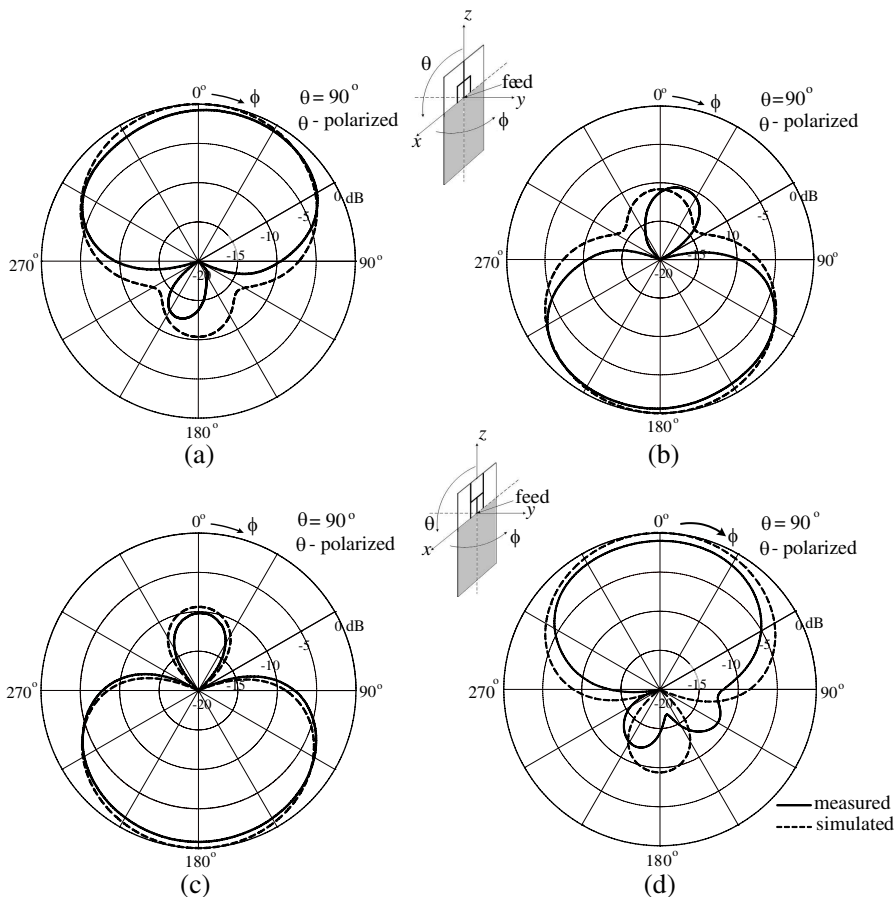


Figure 8. Simulated and measured gain patterns of the antennas with FETs: (a) director-type, FET1, (b) director-type, FET1, (c) reflector-type, FET2, and (d) reflector-type, FET2.

dielectric efficiency

$$e_{cd} = \frac{P_{\text{radiated}}}{P_{\text{accepted}}} = \frac{R_r}{R_L + R_r}$$

where R_r is the radiation resistance, and R_L is the loss resistance [26]. The table shows that the ohmic losses dissipated by the on and off-state resistances range from 1.1–6.4%, and 7.9–10.8%, respectively. This result implies that the antenna efficiency could be increased by 9.4–15.3% by utilizing the ideal switches ($0\ \Omega$ for on and $\infty\ \Omega$ for off). Note that due to the loss from the substrate, the efficiency of the antennas for both types with ideal switches is observed to be imperfect, ranging from 81.4 to 88.0%. Presently, micro-electro-mechanical

Table 3. Measured maximum gain and FBR of antennas with PIN diodes and FET switches.

Antenna type	Switch type	Max gain	Max gain	FBR	FBR
		Bias 1	Bias 2	Bias 1	Bias 2
Director type	PIN	1.18 dB	0.18 dB	7.78 dB	6.55 dB
	FET	0.81 dB	0.97 dB	13.00 dB	10.63 dB
Reflector type	PIN	0.22 dB	-0.03 dB	14.48 dB	17.39 dB
	FET	0.11 dB	-0.29 dB	9.63 dB	13.42 dB

*Bias1: forward bias (PIN diodes), FET1 on (FET's).

Bias2: reverse bias (PIN diodes), FET2 on (FET's).

Table 4. Computed efficiency for the antennas switched by PIN diodes and FETs versus on and off-state resistance.

Antenna type	Switch type	Eq.	R_{on}	R_{off}	$R_{on} = 0 \Omega$
		circuit [%]	$= 0 \Omega$ [%]	$= \infty \Omega$ [%]	$R_{off} = \infty \Omega$ [%]
Director type	PIN	74.4	75.5	84.3	85.7
	FET	70.0	76.4	77.9	85.3
Reflector type	PIN	78.6	79.9	87.1	88.0
	FET	69.4	71.0	80.2	81.4

*Bias1: forward bias (PIN diodes), FET1 on (FET's).

Bias2: reverse bias (PIN diodes), FET2 on (FET's).

switches (MEMS) may be the closest to ideal switches among tunable switching devices that can be used in mobile communications since they offer relatively lower power dissipation, being implemented in smaller packages [27, 28]. In particular, capacitive-type MEMS switches show especially low ohmic losses, which may result in a significant increase in the antenna efficiency [29]. However, the reliability of the MEMS switches remains a problem [30]. In addition, managing the bias network including the DC control lines is another important issue since an inadequately-located bias network may weaken the beam pattern reconfiguration. When using PIN diodes, the DC control signal is supplied in combination with the RF signal, thereby minimizing the effect originating from the bias network. Thus, in this case, the performance of the DC blocking device becomes critical in radiation efficiency. On the other hand, when using FET switches, separate control lines are required. As the bias lines used in the proposed antennas are loaded with a 500Ω resistor, they have advantage of being electromagnetically transparent, minimizing the radiation

pattern disturbance. Lastly, in view of power management, FET switches are more advantageous than PIN diodes since the FETs draw essentially no DC current, while PIN diodes draw DC current to switch into the on state, increasing battery power consumption.

5. CONCLUSION

In this paper, two types of symmetric beam pattern-reconfigurable antennas were designed to operate over DCS 1800 frequency bands. The electrical shapes of both the antenna structures are symmetric with respect to the vertical center axis, consisting of a monopole-loaded loop and an open wire. The open wire serves as either director or reflector for the two types of antenna. Depending on the switching state, the antennas choose between the two symmetric beam directions while maintaining their input impedance, which is the salient characteristic of radiation pattern-reconfigurable antennas. Using equivalent linear circuit models, sizes of the proposed antennas with the PIN diodes and FETs are then optimized to achieve beam switching capability. Next, the reflection coefficients and gain patterns under different bias conditions using both switches are measured and compared with the simulated results. The measured results indicate that the two proposed antennas can clearly alternate their radiation patterns using tunable switching devices, with no input impedance difference.

ACKNOWLEDGMENT

This work was supported by the Unmanned Technology Research Center, Defense Acquisition Program Administration, and Agency for Defense and Development, Daejeon, Korea.

REFERENCES

1. Sun, L., B.-H. Sun, J.-Y. Li, Y.-H. Huang, and Q.-Z. Liu, "Reconfigurable circularly polarized microstrip antenna without orthogonal feeding network," *Journal of Electromagnetic Waves and Applications*, Vol. 25, No. 10, 1352–1359, 2011.
2. Choi, J. and S. Lim, "Frequency and radiation pattern reconfigurable small metamaterial antenna using its extraordinary zeroth-order resonance," *Journal of Electromagnetic Waves and Applications*, Vol. 24, Nos. 14–15, 2119–2127, 2010.
3. Kamarudin, M. R. B., P. S. Hall, F. Colombel, and M. Himdi, "Electronically switched beam disk-loaded monopole array

- antenna,” *Progress In Electromagnetics Research*, Vol. 101, 339–347, 2010.
4. Jamlos, M. F., O. A. Aziz, T. A. Rahman, M. R. Kamarudin, P. Saad, M. T. Ali, and M. N. Md Tan, “A beam steering radial line slot array antenna with reconfigurable operating frequency,” *Journal of Electromagnetic Waves and Applications*, Vol. 24, Nos. 8–9, 1079–1088, 2010.
 5. Jamlos, M. F., O. A. Aziz, T. A. Rahman, M. R. Kamarudin, P. Saad, M. T. Ali, and M. N. Md Tan, “A reconfigurable radial line slot array (RLSA) antenna for beam shape and broadside application,” *Journal of Electromagnetic Waves and Applications*, Vol. 24, Nos. 8–9, 1171–1182, 2010.
 6. Lin, S.-Y., Y.-C. Lin, and J.-Y. Lee, “T-strip fed patch antenna with reconfigurable polarization,” *Progress In Electromagnetics Research Letters*, Vol. 15, 163–173, 2010.
 7. Razali, A. R. and M. E. Bialkowski, “Reconfigurable coplanar inverted-F antenna with electronically controlled ground slot,” *Progress In Electromagnetics Research B*, Vol. 34, 63–76, 2011.
 8. Ali, M. T., M. N. M. Tan, A. R. B. Tharek, M. R. B. Kamarudin, M. F. Jamlos, and R. Sauleau, “A novel of reconfigurable planar antenna array (RPAA) with beam steering control,” *Progress In Electromagnetics Research B*, Vol. 20, 125–146, 2010.
 9. Ramadan, A., K. Y. Kabalan, A. El-Hajj, S. Khoury, and M. Al-Husseini, “A reconfigurable U-koch microstrip antenna for wireless applications,” *Progress In Electromagnetic Research*, Vol. 93, 355–367, 2009.
 10. Alkanhal, M. A. S. and A. F. Sheta, “A novel dual-band reconfigurable square-ring microstrip antenna,” *Progress In Electromagnetic Research*, Vol. 70, 337–349, 2007.
 11. Shynu, S. V., G. Augustin, C. K. Aanandan, P. Mohanan, and K. Vasudevan, “Design of compact reconfigurable dual frequency microstrip antennas using varactor diodes,” *Progress In Electromagnetic Research*, Vol. 60, 197–205, 2006.
 12. Abdallah, M., F. Colombel, G. Le Ray, and M. Himdi, “Frequency tunable antenna for digital video broadcasting handheld application,” *Progress In Electromagnetic Research Letters*, Vol. 24, 1–8, 2011.
 13. Monti, G., L. Corchia, and L. Tarricone, “Planar bowtie antenna with a reconfigurable radiation pattern,” *Progress In Electromagnetic Research C*, Vol. 28, 61–70, 2012.
 14. Kelly, J. R., P. Song, P. S. Hall, and A. L. Borja, “Reconfigurable

- 460 MHz to 12 GHz antenna with integrated narrowband slot,” *Progress In Electromagnetic Research C*, Vol. 24, 137–145, 2011.
15. Nikolau, S., R. Bairavasubramanian, C. Lugo, Jr., I. Carrasquillo, D. C. Thompson, G. E. Ponchak, J. Papapolymerou, and M. M. Tentzeris, “Pattern and frequency reconfigurable annular slot antenna using PIN diodes,” *IEEE Trans. on Antennas and Propagat.*, Vol. 54, 439–448, 2006.
 16. Huff, G. H., J. Feng, S. Zhang, and J. T. Bernhard, “A novel radiation pattern and frequency reconfigurable single turn square spiral microstrip antenna,” *IEEE Microwave Wireless Components Lett.*, Vol. 13, 57–59, 2003.
 17. Yang, X.-S., B.-Z. Wang, W. Wu, and S. Xiao, “Yagi patch antenna with dual-band and pattern reconfigurable characteristics,” *IEEE Antennas Wireless Propagat. Lett.*, Vol. 6, 168–171, 2007.
 18. Zhang, S., G. H. Huff, J. Feng, and J. T. Bernhard, “A Pattern reconfigurable microstrip parasitic array,” *IEEE Trans. on Antennas and Propagat.*, Vol. 52, 2773–2776, 2004.
 19. Yu, Z.-W., G.-M. Wang, X.-J. Gao, and K. Lu, “A novel small-size single patch microstrip antenna based on koch and Sierpinski fractal-shapes,” *Progress In Electromagnetic Research Letters*, Vol. 17, 95–103, 2010.
 20. 3GPP TS 05.05 version 8.20.0 Release 1999 Pages 9 and 10.
 21. Kwon, D. H. and Y. Kim, “Small low-profile loop wideband antennas with unidirectional radiation characteristics,” *IEEE Trans. on Antennas and Propagat.*, Vol. 55, 72–77, 2007.
 22. MPP4203 datasheet, Available at www.microsemi.com.
 23. ATF-34143 datasheet, Available at www.home.agilent.com.
 24. Pringle, L. N., P. H. Harms, S. P. Blalock, G. N. Kiesel, E. J. Kuster, P. G. Friederich, R. J. Prado, J. M. Morris, and G. S. Smith, “A Reconfigurable aperture antenna based on switched links between electrically small metallic patches,” *IEEE Trans. on Antennas and Propagat.*, Vol. 52, 1434–1445, 2004.
 25. Peroulis, D., K. Sarabandi, and L. P. B. Katehi, “Design of reconfigurable slot antennas,” *IEEE Trans. on Antennas and Propagat.*, Vol. 53, 645–654, 2005.
 26. Balanis, C. A., *Antenna Theory*, John Wiley and Sons, Hoboken, 2005.
 27. Goldsmith, C., J. Randall, S. Eshelman, T. H. Lin, D. Denniston, S. Chen, and B. Norvell, “Characteristics of micromachined switches at microwave frequencies,” *IEEE Microwave Theory and*

- Techniques Symp. Dig.*, Vol. 2, 1141–1144, 1996.
28. Pacheco, S., L. P. B. Katehi, and C. T. Nguyen, “Design of low actuation RF MEMS switch,” *IEEE Microwave Theory and Techniques Symp. Dig.*, Vol. 1, 165–170, 2000.
 29. Muldavin, J. B. and G. M. Rebeiz, “High-isolation CPW MEMS shunt switches — Part 2: Design,” *IEEE Trans. on Microwave Theory and Techniques*, Vol. 48, 1053–1056, 2000.
 30. Jung, C. W., Y. J. Kim, Y. E. Kim, and F. D. Flaviis, “A macro-micro frequency tuning antenna for the reconfigurable wireless communication systems,” *Electron. Lett.*, Vol. 43, 201–202, 2007.